Cell, Vol. 120, 843–856, March 25, 2005, Copyright ©2005 by Elsevier Inc. DOI 10.1016/j.cell.2005.01.008

Perp Is a p63-Regulated Gene Essential for Epithelial Integrity

Rebecca A. Ihrie,[1,2] Michelle R. Marques,[1,2] Bichchau T. Nguyen,[1,2] Jennifer S. Horner,[1,2] Cristian Papazoglu,[4,5] Roderick T. Bronson,[6] Alea A. Mills,[4] and Laura D. Attardi[1,2,3,*]

[1]Division of Radiation and Cancer Biology
[2]Department of Radiation Oncology
[3]Department of Genetics
Stanford University School of Medicine
Stanford, California 94305
[4]Cold Spring Harbor Laboratory
Cold Spring Harbor, New York 11724
[5]Graduate Program in Genetics
Stony Brook University
Stony Brook, New York 11794
[6]Department of Pathology
Harvard Medical School
Boston, Massachusetts 02115

Summary

p63 is a master regulator of stratified epithelial development that is both necessary and sufficient for specifying this multifaceted program. We show here that Perp, a tetraspan membrane protein originally identified as an apoptosis-associated target of the p53 tumor suppressor, is the first direct target of p63 clearly involved in mediating this developmental program in vivo. During embryogenesis, Perp is expressed in an epithelial pattern, and its expression depends on p63. *Perp*$^{-/-}$ mice die postnatally, with dramatic blistering in stratified epithelia symptomatic of compromised adhesion. Perp localizes specifically to desmosomes, adhesion junctions important for tissue integrity, and numerous structural defects in desmosomes are observed in Perp-deficient skin, suggesting a role for Perp in promoting the stable assembly of desmosomal adhesive complexes. These findings demonstrate that Perp is a key effector in the p63 developmental program, playing an essential role in an adhesion subprogram central to epithelial integrity and homeostasis.

Introduction

The genesis of a specialized tissue from a simple germ layer relies on the implementation of elaborate transcriptional programs (Fuchs and Raghavan, 2002). p63, a member of a family of transcription factors including the p53 tumor suppressor, plays a vital role in the development of stratified epithelia. Mice lacking p63 display postnatal lethality with a dramatic absence of limbs and skin due to the failure of these epithelia to develop during gestation (Mills et al., 1999; Yang et al., 1999). Ectopic expression of p63 in simple epithelia in vivo is sufficient to initiate critical aspects of stratification, suggesting that p63 performs an instructive role in this developmental program (Koster et al., 2004). Although these findings underscore the essential nature of p63 function in the determination of stratified epithelia, the specific pathways by which p63 acts are unknown.

The best characterized of the stratified epithelia is the epidermis of the skin, a self-renewing organ that regenerates approximately every 2 weeks (Fuchs and Raghavan, 2002). In skin, the basal cells of the innermost layer of the epidermis constitute the proliferative compartment renewing the epidermis. Progenitor cells of this basal layer, called transit amplifying cells, divide several times before withdrawing from the cell cycle, detaching from the basement membrane, and embarking on a migration and differentiation program. This differentiation process culminates with the formation of a keratinized cell layer, the stratum corneum, which provides a protective surface that also serves a barrier function. Although the extent of p63 protein expression throughout the skin is not completely characterized, p63 is certainly expressed in the basal layer, where it is poised to influence early steps of stratified epithelial development (McKeon, 2004).

Among the specializations most critical for stratified epithelial formation are cell-cell adhesive complexes including adherens junctions, tight junctions, and desmosomes (Green and Gaudry, 2000). These intercellular junctions promote interaction between epithelial cells, facilitating the mechanical linkage of cells or barrier function. Desmosomes are specialized adhesive junctions that are particularly important for the structural integrity of tissues subject to mechanical stress, such as the skin or the oral epithelia (Getsios et al., 2004). Desmosomes assemble when the transmembrane desmosomal cadherins interact to bring the plasma membranes of adjacent cells in close apposition and nucleate cytoplasmic complexes of plakoglobin, plakophilin, and desmoplakin to form a structure called the desmosomal plaque. Through linkage of the plaque to the keratin intermediate filament cytoskeleton via desmoplakin, desmosomes allow the formation of a supracellular network that endows an epithelium with strength and resiliency. The crucial role of desmosomal proteins in tissue integrity is underscored by the various human blistering diseases resulting from defects in desmosomal function (Green and Gaudry, 2000).

How p63 might implement subprograms fundamental to stratified epithelial development and integrity, including adhesion, proliferation, and polarity, is unknown. p63 may transactivate a cohort of genes that determine the identity and structure of stratified epithelia, but to date, p63 target genes clearly involved in stratified epithelial function in vivo have not been identified (Dohn et al., 2001; Ellisen et al., 2002; Kurata et al., 2004). Several characteristics of the gene *Perp* (p53 effector related to PMP-22) make it a compelling candidate for such a target. *Perp* is a p53 target gene involved in DNA damage-induced apoptosis, and during this pro-

*Correspondence: attardi@stanford.edu

cess, the *Perp* promoter is bound not only by p53 but also by p63, indicating that Perp is responsive to signals from p63 (Flores et al., 2002; Ihrie et al., 2003). Moreover, *Perp* is unique among p53 targets because it encodes a tetraspan membrane protein, implicating it in cell-cell interactions. Although Perp's exact molecular function is unknown, it is distantly related to members of the claudin/PMP-22/EMP family of four-pass membrane proteins (Attardi et al., 2000). This multiprotein family includes stargazin, claudins, and PMP-22, which participate in a variety of cellular processes including ion channel function, receptor trafficking, tight junction formation, and myelination (Jetten and Suter, 2000; Tsukita and Furuse, 2002). As a plasma membrane protein, Perp could act in a manner similar to any of these proteins to affect events important for tissue development or architecture.

Here, we demonstrate that Perp is a principal player in the p63-directed program of stratified epithelial development. We show that Perp displays a striking epithelial-specific expression pattern during embryogenesis and that its expression depends on direct activation by p63. Through the characterization of *Perp*$^{-/-}$ mice, we determine that Perp has a pivotal role in cell-cell adhesion by enabling desmosome function. These studies identify Perp as the first direct molecular target of p63 definitively involved in stratified epithelial function in vivo. Our results provide an initial understanding of the subprograms dictating specific tissue attributes downstream of p63, a global regulator of epithelial development, integrity, and homeostasis.

Results

Perp Is Highly Expressed in Stratified Epithelia

To elucidate the developmental role for Perp in vivo as a potential target of p63, we began by determining the spatial localization pattern of *Perp* mRNA during embryogenesis. In early embryos (E9.5–10.5), *Perp* mRNA expression was observed in the ectoderm of the developing branchial arches and limb buds, as well as in surface ectoderm, by whole-mount in situ hybridization (Figures 1A and 1B and data not shown). At later stages of development (E16.5–18.5), *Perp* mRNA localized predominantly to epithelia, most notably the oral mucosa and skin (Figure 1G). Analysis of Perp protein levels in a variety of adult mouse tissues by Western blot and immunohistochemistry confirmed its expression in stratified epithelia, including the skin and tongue, but not in simple epithelia (Figure 1H and see Figure S2H in the Supplemental Data available with this article online; data not shown). To determine the profile of Perp protein expression during the conversion of ectoderm to stratified epidermis, which occurs from approximately E9.5–E15.5, we performed immunohistochemical analysis (Figure 1I). We found Perp protein expressed in developing skin during and after the stratification process, consistent with a role for Perp in this compartment.

Perp Is a p63 Target Gene

The pattern of *Perp* mRNA expression in the branchial arches and developing limb buds in a profile coincident with that observed for *p63* mRNA, as well as its specific localization to stratified epithelia, suggested Perp might be a target of p63 during epithelial development (Figures 1A, 1B, and 1I; Mills et al., 1999; Yang et al., 1999). To test this hypothesis, we analyzed *Perp* mRNA expression in E9.5 *p63*$^{-/-}$ embryos, before the defects associated with p63 loss compromised the integrity of the tissues that express *Perp*. We found that *Perp* mRNA was absent from the limb buds and branchial arches in *p63*$^{-/-}$ embryos (Figures 1C and 1E) but was unaltered in *p53*$^{-/-}$ embryos (Figure 1D). Consistent with these results, Northern blot analysis demonstrated that *Perp* mRNA is present in both wild-type and *p53*$^{-/-}$, but not *p63*$^{-/-}$, E14.5 body tissue (Figure 2A). The absence of *Perp* expression is specifically due to p63-deficiency and not a lack of the appropriate tissue specified by p63, as RNA interference experiments showed that ablation of p63 in primary mouse keratinocytes results in severely diminished *Perp* expression (Figures 2B and 2C). Together, these findings indicate that *Perp* expression during embryogenesis requires the presence of p63, but not p53, and are consistent with the idea that *Perp* is a key target of p63 in maturing stratified epithelia.

To determine if p63 directly regulates *Perp* expression, we pursued several approaches. We first tested whether p63 could transactivate a reporter construct comprising the *Perp* promoter and a segment of the first intron fused to luciferase. To eliminate background effects of endogenous p63 or p53, we introduced p63 expression constructs into *p63*$^{-/-}$;*p53*$^{-/-}$ MEFs along with the *Perp* reporter construct (Figure 2D). p63 exists in multiple forms, including transactivating (TA) isoforms and ΔN isoforms lacking amino-terminal transactivation sequences, each transcribed from distinct promoters (Yang et al., 1998). Moreover, each of these isoforms can be alternatively spliced to yield the α, β, and γ variants. As the roles of each isoform in vivo may differ, we tested several isoforms in our assays. We found that TAp63α and TAp63γ both robustly transactivated the *Perp* reporter construct, and this was mediated largely through the p53/p63 consensus element in intron 1, the major p53-responsive site in *Perp* (Figure 2D; Reczek et al., 2003). The ΔNp63 isoforms also transactivated the reporter efficiently, to levels similar to or greater than those observed for p53. The ability of p63 to induce the *Perp* reporter was confirmed through experiments in wild-type keratinocytes, which indicated that both TAp63 and ΔNp63 isoforms can directly activate *Perp* expression in cells where p63 exerts its function, with ΔN isoforms activating to levels ~50% of those seen with TAp63 isoforms (Figure 2E) . To determine if p63 directly binds the *Perp* endogenous regulatory region in vivo, we performed chromatin immunoprecipitation (ChIP) assays (Figure 2F). We found that p63 protein in newborn mouse skin binds the intron 1 p53/p63 site, the key p63-responsive element in the *Perp* regulatory region. Further support of the idea that p63 is a major regulator of *Perp* was provided by experiments showing that TAp63γ expression is sufficient to drive endogenous *Perp* mRNA expression in cultured E18.5 *p63*$^{-/-}$ ectodermal cells (Figure 2G). Taken together, these results implicate *Perp* as a direct p63 target gene during skin development.

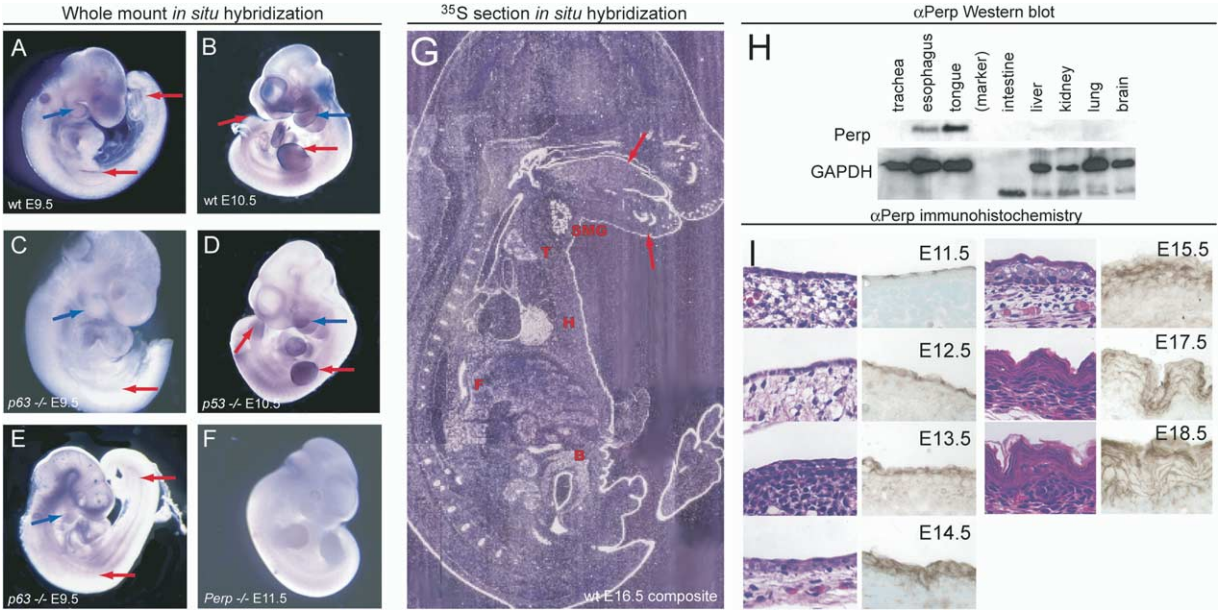

Figure 1. *Perp* Expression During Development

(A and B) *Perp* expression in early embryogenesis (E9.5–10.5) is observed in the apical ectodermal ridge (AER) of the developing limb buds (red arrows) and the branchial arches (blue arrows) by whole-mount in situ hybridization. Digoxigenin-labeled probe localization appears as dark purple precipitate.

(C–E) This pattern of expression is absent in $p63^{-/-}$ embryos (arrows in [C] and [E]) but is present in $p53^{-/-}$ embryos (arrows in [D]).

(F) Detection of *Perp* mRNA is specific, as staining is absent in a *Perp* null embryo.

(G) At E16.5, *Perp* mRNA is localized to many epithelia throughout the embryo by ^{35}S in situ hybridization. Radioactive probe localization appears as white precipitate. *Perp* is highly expressed in the skin (arrow), tongue (arrow), palate, and hair follicles. Additionally, *Perp* mRNA was detected in other tissues, including the heart (H), forestomach (F), submandibular gland (SMG), thymus (T), and bladder (B).

(H) Perp protein is expressed in stratified but not simple epithelia in the adult mouse, as determined by Western blot analysis. GAPDH serves as a loading control.

(I) Perp protein is observed during stratified epithelial development by immunohistochemistry. Skin sections of embryos from E11.5 to E18.5 are shown, with Perp immunohistochemistry marked by brown precipitate at the right of each panel and accompanying H&E staining at the left.

Perp Is Essential for Postnatal Viability

To determine the specific function Perp might perform in the p63 stratified epithelial development program in vivo, we generated *Perp* knockout mice. We deleted exons 2 and 3 of the *Perp* gene, which encode the majority of the protein, in ES cells and used these targeted cells to generate *Perp* heterozygous mutant mice (Figure 3A). Northern blot and immunohistochemistry experiments verified that this *Perp* allele is a null (Figures S2H and S2I; Ihrie et al., 2003). $Perp^{+/-}$ mice were intercrossed, and the frequency of offspring of each genotype was examined at 3 weeks of age (Figure 3B). We examined mice both on a mixed 129/Sv;C57BL/6 background and on a pure 129/Sv background. Whereas these crosses produced wild-type and heterozygous mice in abundance, homozygous mutant mice were drastically underrepresented at weaning, with no *Perp* null mice surviving on a pure 129/Sv background. An extremely limited number of mixed background $Perp^{-/-}$ mice survived until adulthood, but these mice ultimately also exhibited increased mortality (Figure 3B and data not shown).

To establish when *Perp* deficiency compromises viability, we genotyped both embryos and neonatal progeny from *Perp* heterozygote intercrosses. We found that although *Perp* null mice survive until birth, the vast majority die within ten days after birth, with signs of wasting at the time of death (Figures 3C and 3D). This lethal phenotype is in striking contrast to the viability of $p53^{-/-}$ mice (Attardi and Jacks, 1999), suggesting that the role of Perp in development is p53 independent and raising the possibility that the requirement for Perp may reflect instead a specific role as a target of p63 in epithelia.

$Perp^{-/-}$ Mice Display Dramatic Blistering of the Skin and Oral Mucosa

The prominent stratified epithelial pattern of *Perp* expression and its position downstream of p63 suggested a potential role for Perp in these tissues. We therefore focused our initial pathological examination on these epithelial structures to discover the cause of mortality in $Perp^{-/-}$ newborn mice. Although the skin and oral mucosa of postnatal day 0.5 (P0.5) $Perp^{-/-}$ newborns appeared histologically similar to those of wild-type littermates (data not shown), examination of the same tissues in P7.5 $Perp^{-/-}$ mice revealed the presence of severe blisters (Figures 3E–3L). Analysis of the oral cavities of many $Perp^{-/-}$ mice (n = 14) showed multiple blisters of the oral epithelia, as well as thickening of

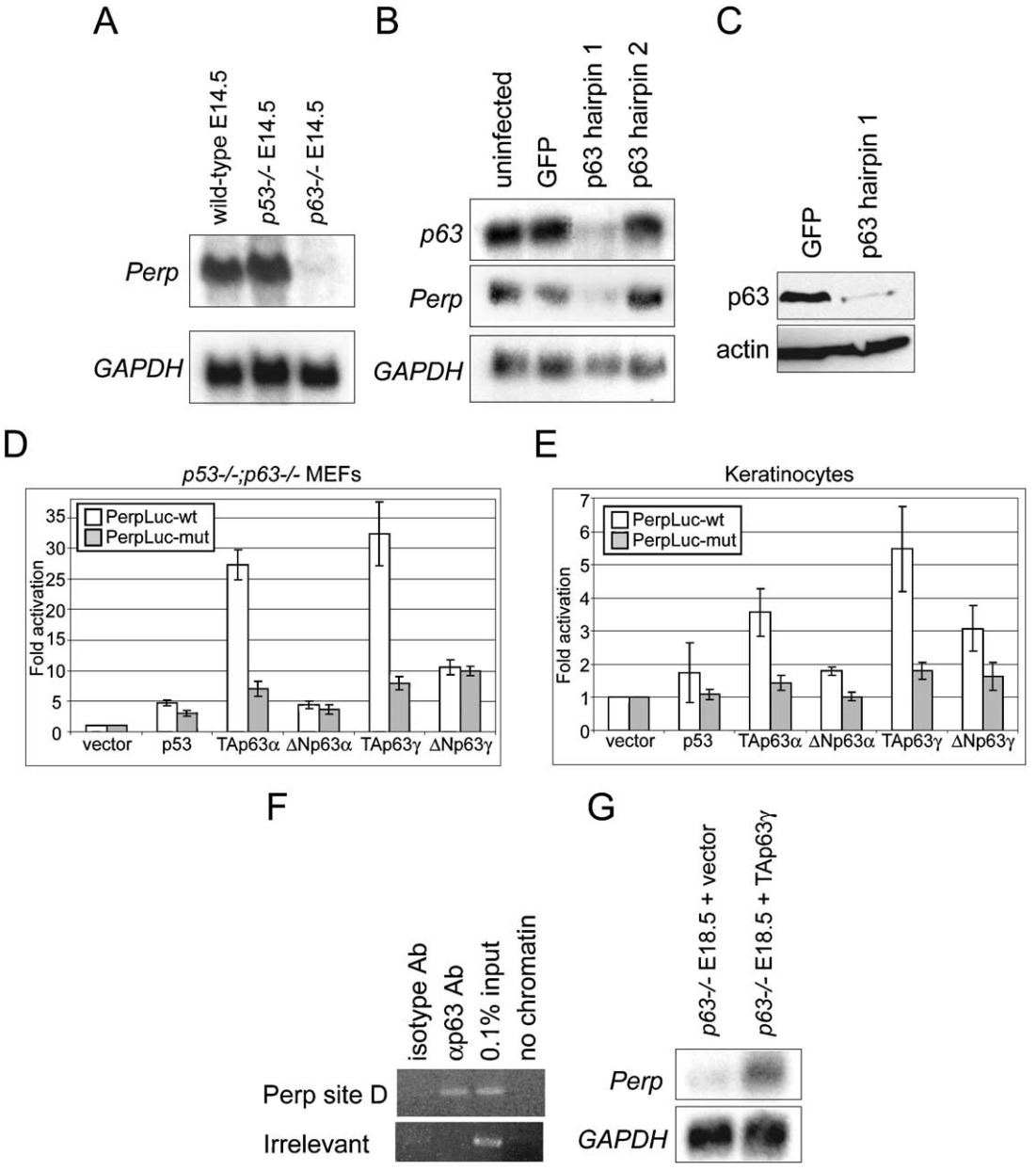

Figure 2. *Perp* Is a p63 Target Gene

(A) Northern blot analysis shows robust *Perp* expression in wild-type and $p53^{-/-}$, but not $p63^{-/-}$, embryonic carcass tissue at E14.5. *GAPDH* serves as a loading control.

(B) p63 is necessary for *Perp* expression in primary mouse keratinocytes. Infection of keratinocytes with retroviruses that do not affect p63 levels (either a GFP-expressing construct or a construct expressing an ineffective short hairpin RNA [shRNA] directed against p63, "p63 hairpin 2") has no effect on *Perp* message levels, as determined by Northern blot. In contrast, expression of an shRNA that severely diminishes p63 mRNA levels ("p63 hairpin 1") sharply reduces *Perp* message levels.

(C) Western blot analysis shows that expression of p63 hairpin 1 efficiently reduces p63 protein levels.

(D) A variety of p63 isoforms are capable of transactivating the *Perp* reporter construct (PerpLuc-wt), consisting of the promoter and part of the first intron fused to luciferase, in luciferase assays performed in $p53^{-/-};p63^{-/-}$ MEFs. Mutation of the intronic p53/p63 binding site in the *Perp* first intron (site D) compromises this transactivation activity (PerpLuc-mut). The graph shows the fold activation of the reporter by the expressed proteins relative to the empty vector and represents the average of three experiments ±SEM.

(E) All p63 isoforms transactivate the wild-type *Perp* luciferase reporter construct in primary human keratinocytes. The average of four experiments ±SEM is shown.

(F) Chromatin immunoprecipitation on newborn mouse skin shows that p63 binds the p53/p63 consensus site in the *Perp* first intron (site D). Ethidium-stained agarose gels show a PCR product encompassing site D upon immunoprecipitation with p63 antibodies but not in a mock immunoprecipitation without chromatin or an immunoprecipitation using an isotype control nonspecific antibody. In addition, no PCR product was observed in the p63 chromatin immunoprecipitation using irrelevant primers for a portion of the *Perp* gene lacking a p53 binding site.

(G) Northern blot analysis demonstrates that *Perp* mRNA is expressed at low levels in cultured E18.5 $p63^{-/-}$ ectoderm but is efficiently induced upon infection with a TAp63γ-expressing adenovirus.

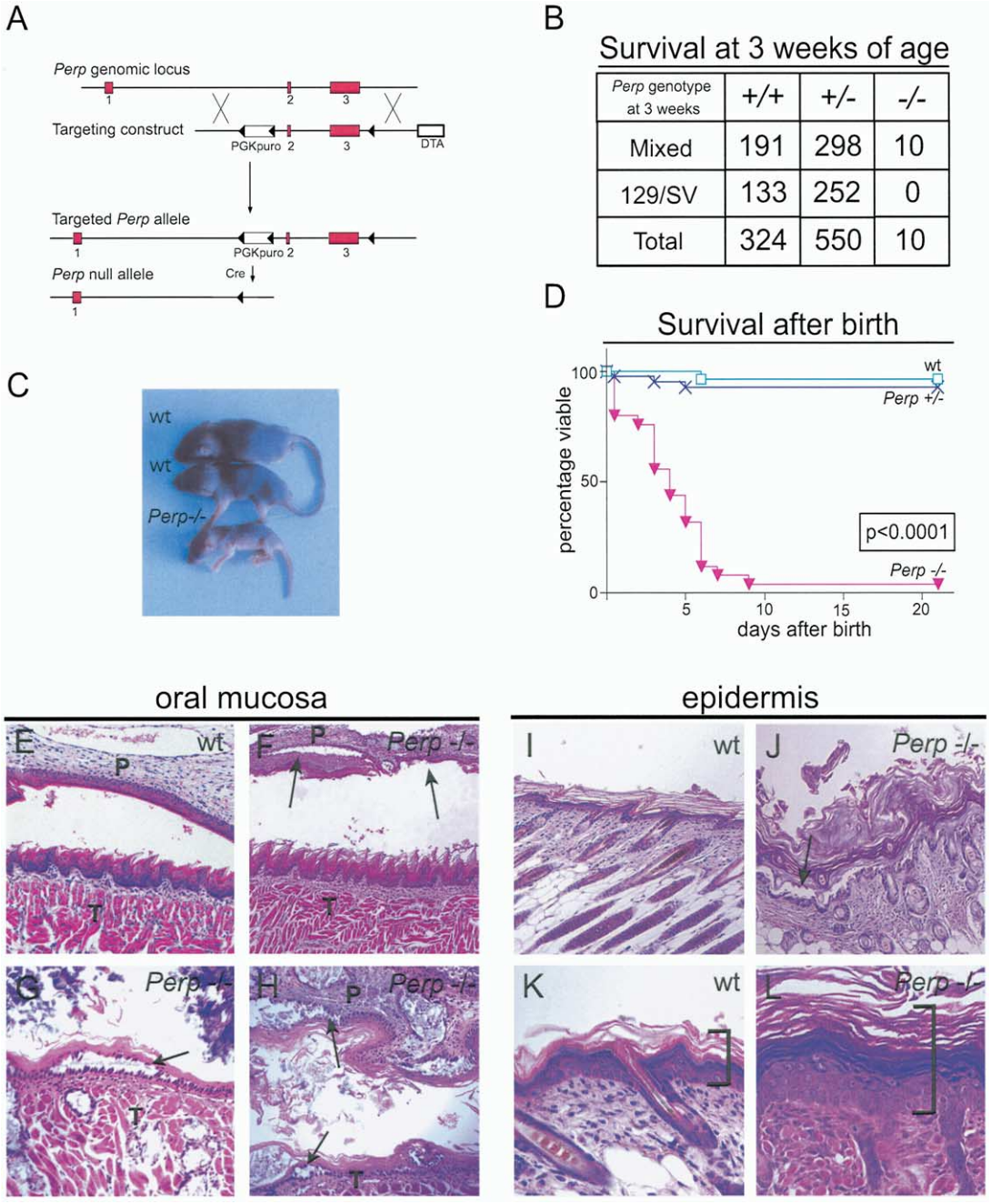

Figure 3. *Perp*$^{-/-}$ Mice Exhibit Postnatal Lethality and Defects in Stratified Epithelia

(A) Targeting scheme for generating *Perp* null mice. A targeting construct in which *Perp* exons 2 and 3 were flanked by *loxP* sites (triangles) was introduced into 129/Sv embryonic stem cells. These exons were then deleted via introduction of Cre recombinase, resulting in a null allele, and ES cells were used to generate *Perp*$^{-/-}$ mice.

(B) Genotypes of 3-week-old progeny derived from *Perp* heterozygote intercrosses. The numbers of wild-type, *Perp*$^{+/-}$ and *Perp*$^{-/-}$ mice observed on either a mixed 129/Sv-C57BL/6 or a pure 129/Sv genetic background are indicated.

(C) Appearance of *Perp* null pups at P5. Whereas wild-type pups appear normal, *Perp*$^{-/-}$ pups show signs of wasting.

(D) Survival of *Perp* null newborns after birth. Kaplan-Meier analysis demonstrates that whereas most wild-type and *Perp*$^{+/-}$ mice survive until weaning, the vast majority of *Perp*$^{-/-}$ mice die within the first week of life.

(E) Wild-type oral mucosa (P, palate and T, tongue) develops normally at P7.5.

(F) In contrast, *Perp*$^{-/-}$ animals exhibit severe lesions in the oral cavity, primarily blisters between the basal and immediate suprabasal layers of the epithelium (arrows).

(G) Higher magnification view of a basal-suprabasal blister in a *Perp*$^{-/-}$ tongue.

(H) Many *Perp*$^{-/-}$ mice exhibit multiple lesions (arrows) as well as debris in the throat.

(I–L) The skin of P7.5 *Perp*$^{-/-}$ mice (J and L) is also aberrant when compared to wild-type littermates (I and K). *Perp*$^{-/-}$ epidermis is thicker than that of wild-type mice (brackets in [K] and [L]) and also exhibits blistering ([J], arrow).

these tissues (Figures 3F–3H). The blisters most commonly observed were splits between the basal and suprabasal layers of cells, often with disrupted adhesion between individual cells, known as acantholysis (Figure 3G). In addition to blistering in the oral mucosa, *Perp*$^{-/-}$ pups exhibited frequent basal-suprabasal blistering in the skin, as well as dramatic thickening of the epidermis (Figures 3J and 3L). These phenotypes highlight a potential function for Perp in epithelial adhesion and provide a rationale for the lethality of *Perp* null newborns. The observed debris in the mouth and throat suggest that the mechanical stress of feeding progressively increases the severity of these blisters, ultimately impeding feeding and leading to the death of the mouse.

To determine if *Perp*$^{-/-}$ mice manifested any other phenotypes typical of *p63* null mice, we examined tissues known to be affected by the absence of p63. *p63*$^{-/-}$ mice are born with craniofacial defects and truncated limbs and lack ectodermal appendages such as teeth. In contrast, *Perp*$^{-/-}$ mice exhibited grossly normal craniofacial, limb, and tooth development (Figures S1A–S1D and data not shown). These findings suggest that Perp's requirement downstream of p63 is most prominent in tissues subject to significant mechanical stress, specifically the stratified epithelia of the skin and oral mucosa.

Apoptosis and Differentiation Are Unaltered in *Perp*-Deficient Epithelia

Perp's function in epithelial integrity could reflect its known role in apoptosis (Ihrie et al., 2003) or a novel, direct role in adhesion. We first examined apoptosis and proliferation in the *Perp*$^{-/-}$ newborn epithelia to determine if the observed blistering might be due to altered tissue homeostasis. Virtually no apoptotic cells were observed in either wild-type or *Perp*$^{-/-}$ skin using TUNEL staining (Figures S2A and S2B). *Perp*$^{-/-}$ skin did exhibit increased staining for the proliferation marker Ki67 relative to wild-type skin in the basal layer of interfollicular epidermis (Figures S2C, S2D, and S2G), suggesting that the abnormal thickness of *Perp*$^{-/-}$ skin is directly due to hyperproliferation. *Perp*$^{-/-}$ skin also exhibited broad staining for keratin 6 (Figures S2E and S2F), which is frequently induced in the interfollicular epidermis in response to adhesion defects, hyperproliferative signals, or wounding (Wong et al., 2000). This finding suggests that the enhanced proliferation observed in the *Perp*$^{-/-}$ mice could reflect a response to an adhesion defect rather than a cause. Despite this hyperproliferation, terminal differentiation markers appeared unaltered in *Perp*$^{-/-}$ skin when compared to wild-type skin, suggesting that neither the thickening nor the blistering phenotypes seen in *Perp*$^{-/-}$ skin are due to a differentiation defect (Figures S2J–S2O). In light of these data, we designed experiments to elucidate what direct role Perp might play in cell-cell adhesion.

Perp Localizes to Desmosomes

To investigate the function of Perp in adhesion, we began by studying the subcellular localization of Perp in newborn skin. Indirect immunofluorescence using antibodies directed against Perp demonstrated that it is highly expressed in all layers of the skin. Closer examination of this staining pattern showed that Perp localizes to the plasma membrane and exhibits a punctate pattern similar to that observed with other adhesion proteins (Figures 4A and 4B).

Proper cell-cell adhesion in the skin requires the presence of multiple adhesion complexes, including adherens junctions, desmosomes, and tight junctions (Fuchs and Raghavan, 2002). The punctate pattern of Perp staining suggested a potential association with one or more of these complexes. To distinguish these possibilities, we utilized Madin Darby canine kidney (MDCK) epithelial cells, a well-characterized model system for examining intercellular junctions in polarized epithelial layers (Yeaman et al., 2004). Cells were transfected with a construct encoding a Perp-GFP fusion protein before formation of a polarized confluent monolayer. By confocal microscopy, we found that overexpressed Perp-GFP did not colocalize with the tight junction protein ZO-1 (Figures S3C and S3D) but showed some colocalization with both the desmosomal protein desmoplakin (Figure S3A) and the adherens junction protein E-cadherin (Figure S3B).

To distinguish the two possible junctions that might contain Perp, we turned to immunogold electron microscopy (EM) on newborn skin, which allowed us to examine the precise localization of endogenous protein in vivo. The electron-dense structure of the desmosome is easily distinguishable by EM, and we found that the gold particles indicating Perp staining localized almost exclusively to the desmosome (Figures 4D and 4E) and were entirely absent from other regions of cell-cell contact (Figure 4G). These experiments demonstrate that endogenous Perp protein localizes specifically to the desmosome.

Desmosome Structure Is Perturbed in *Perp* Null Mice

The localization of Perp to the desmosome suggested that Perp may be important for function of the desmosome, which plays a central role in epithelial integrity and resiliency by linking cell-cell contact points to the keratin cytoskeleton and enhancing the ability of a tissue to resist stress. Consistent with this idea, mice deficient for other desmosomal components exhibit blistering symptoms histologically similar to those seen in *Perp*$^{-/-}$ mice (Koch et al., 1997). Moreover, the desmosomal cadherins desmoglein 1 and 3 are the primary antigens in the human autoimmune blistering diseases pemphigus foliaceus and pemphigus vulgaris, respectively, and patients with these diseases also develop blisters resembling those in *Perp*$^{-/-}$ mice (Green and Gaudry, 2000). We therefore examined the desmosomes in the skin and tongue from *Perp*$^{-/-}$ newborns closely for structural abnormalities.

By EM, desmosomes are highly electron-dense structures and typically appear as two adjacent dark plaques that partially or totally obscure the cellular membrane (red arrows, Figure 5A). In addition, the connection of the desmosomal plaque to the keratin intermediate filaments, which are also electron-dense and therefore distinguishable by EM, often can be visual-

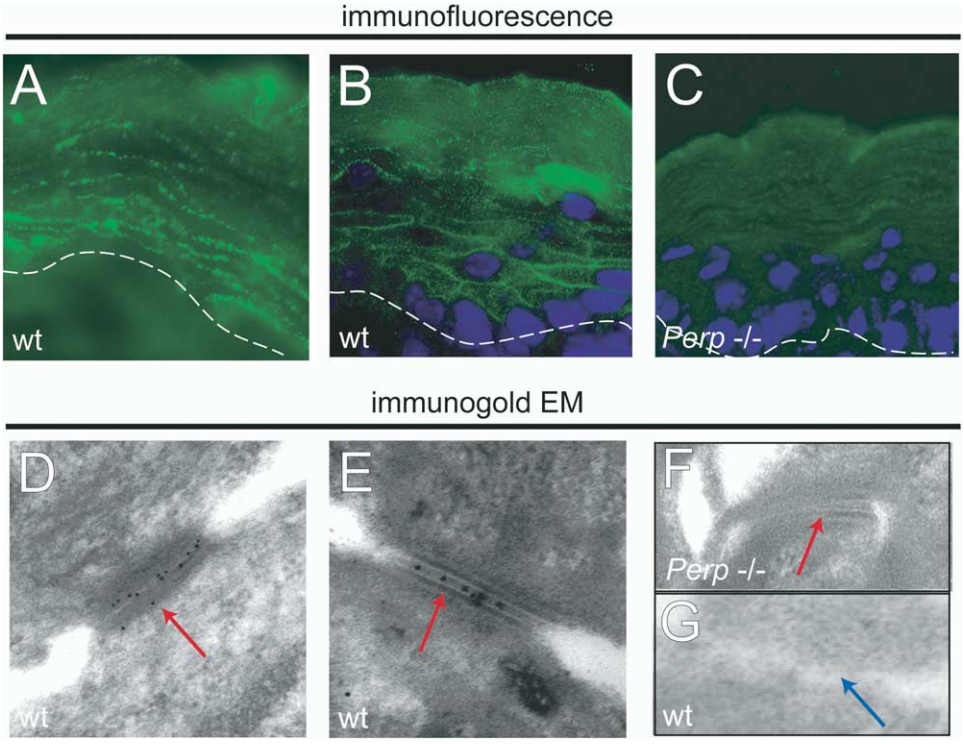

Figure 4. Perp Protein Localizes to the Desmosome

(A and B) Indirect immunofluorescence on P0.5 wild-type skin with anti-Perp antibodies reveals a punctate pattern of staining at the cell membrane. In (B), DAPI staining indicates the basal (nucleated) layer of the epidermis. Dashed lines indicate the basement membrane of the epidermis.

(C) This staining is absent in *Perp*$^{-/-}$ mouse skin.

(D–F) Immunogold EM using anti-Perp antibodies shows that Perp localizes specifically to desmosomes in P0.5 wild-type mouse skin (D and E), but not in *Perp*$^{-/-}$ mouse skin (F).

(G) Perp staining is absent from other regions of cell-cell contact (blue arrows), confirming specific localization to desmosomes.

ized. We focused our analysis on the basal and immediate suprabasal layers of skin, where the most severe blisters were evident in *Perp*$^{-/-}$ mice. At low magnification, some of the blisters present by histology were visible by EM (arrows, Figures S4B and S4C). To assess the state of desmosomes in *Perp*$^{-/-}$ mouse skin, we scored them according to several morphometric criteria: (1) linear density (the number of desmosomes per μm of cellular membrane); (2) the average width of each desmosome, a property thought to reflect the assembly and organization of the desmosome; (3) the electron density of the desmosome relative to the adjoining plasma membrane, which likely indicates the protein content or assembly of the desmosome; (4) the attachment of the desmosome to intermediate filaments; and (5) any other abnormalities, such as obvious detachment from one of the two apposing plasma membranes. Based on meeting these criteria, individual desmosomes were scored as normal or abnormal (Figure 5G).

Whereas desmosomes in wild-type skin appear very electron dense compared to the plasma membrane (red arrows, Figure 5A) and frequently exhibit clear connections to the intermediate filaments (blue arrow, Figure 5A), we found that desmosomes in *Perp* null skin are typically abnormal. Desmosomes in *Perp*$^{-/-}$ skin are wider (Figure 5G), less electron dense (Figure 5B), rarely exhibit clear connections to the cytoskeleton (Figures 5B, 5C, and 5E), and appear at a lower frequency (per μm) than in wild-type skin. In addition, some desmosomes in *Perp* null skin exhibit severe defects in their ability to function as stable cell-cell junctions: the desmosome remains intact and attached to one cell with only a fragment of the apposing cell membrane in evidence (Figures 5C and 5E). This may represent a defect in attachment of the plaque to the intermediate filament network. These abnormalities are quantified in Figure 5G and were observed in multiple *Perp* null mice (n = 4) in comparison to wild-type littermates (n = 2). Similar defects were also observed in the upper suprabasal layer of the skin (data not shown) and in *Perp* null tongue epithelium (n = 4 mice, Figure 5F), suggesting common underlying causes for the blistering in both tissues. In contrast, examination of adherens junctions in *Perp*$^{-/-}$ skin failed to reveal obvious aberrations (data not shown). These data suggest that, while some desmosomes are able to form in the absence of Perp, the desmosomal proteins do not associate as tightly with each other as they do normally and are defective in their ability to form stable attachments to the cytoskeleton. Because the desmosomes in *Perp* null skin are compromised in their strength and organization, epithe-

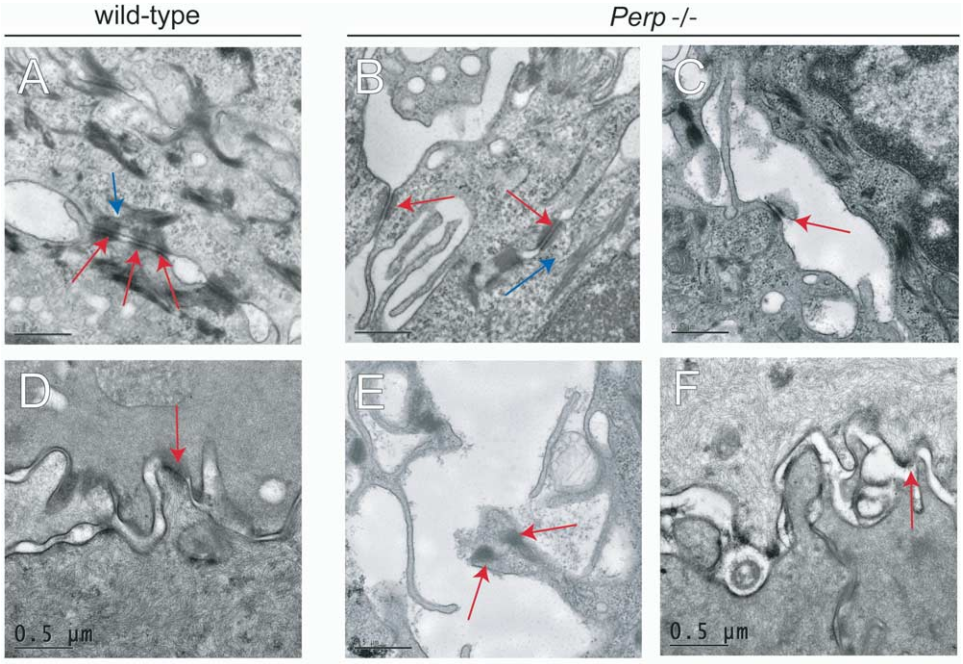

G. Quantitation of skin desmosome properties

genotype (number counted)	desmosomes per μm *	average width (μm) ‡	percentage attached to IF	percentage decreased density	percentage abnormal
wild-type (107)	0.77 ± 0.11	0.19 ± 0.009	85.9	16.8	4.7
Perp-/- (74)	0.50 ± 0.08	0.22 ± 0.016	43.2	58	77

* p = 0.05 and ‡ p = 0.03, unpaired t test

Figure 5. Epithelia From *Perp*$^{-/-}$ Mice Exhibit Aberrant Desmosomes

(A) Wild-type mouse skin contains many desmosomes that are identifiable by EM (red arrows) and show connections to the intermediate filaments (blue arrow).

(B, C, and E) By contrast, desmosomes are less frequent in *Perp*$^{-/-}$ mouse skin and also exhibit other abnormalities, including decreased electron density (red arrows, [B]), lack of attachment to intermediate filaments (blue arrow, [B]), and evident lack of mechanical integrity demonstrated by their detachment from one of the apposed cells (arrows, [C] and [E]).

(D) Normal desmosomes are also present in the wild-type tongue.

(F) Desmosome abnormalities are also present in *Perp*$^{-/-}$ mouse tongue (arrow) when compared to wild-type tongue.

(G) The properties of desmosomes in wild-type and *Perp*$^{-/-}$ mouse skin are quantified in the table shown. Error values in the second and third columns represent the SEM. In total, a high percentage of desmosomes in *Perp*$^{-/-}$ mouse skin was scored as abnormal based on lack of connection to keratin filaments, decreased electron density, or loss of adhesive function.

lia in these mice are greatly susceptible to damage after mechanical stress.

Desmosomal Complexes are Defective in the Absence of Perp

The compromised desmosome function in *Perp* null animals could be explained by deficiencies in levels, localization, or plasma membrane organization of desmosomal constituents. Proteins stably incorporated into the desmosome are characterized by their resistance to solubilization by detergents such as Triton X-100, and therefore increased solubility of desmosomal cadherins or plaque proteins often reflects improper complex assembly (South et al., 2003). However, desmoplakin, which links the desmosomal plaque to the keratin cytoskeleton, is known to exist in Triton X-100-insoluble cytoplasmic bodies prior to desmosome assembly (Green and Gaudry, 2000), and its properties cannot be assessed clearly by solubility assays. We therefore employed both immunofluorescence and biochemical assays to investigate the cause of the desmosome defects observed in *Perp*$^{-/-}$ skin by EM.

We began our analysis of desmosomal components by examining desmosome protein localization in a cell culture model of adhesion. Primary keratinocytes can be induced to form epithelial sheets in culture through a switch from low to high calcium-containing media (Vasioukhin et al., 2001). After 48 hr in high calcium medium, keratinocytes express high levels of desmosomal proteins which complex at the plasma membrane in the form of mature desmosomes. We derived epidermal keratinocytes from P0.5 wild-type and *Perp*$^{-/-}$ mice and examined the subcellular localization of desmosomal proteins after induction of desmosome formation (Figure 6). Although *Perp*$^{-/-}$ keratinocytes exhibit increased levels of multiple desmosomal proteins (Figures 7A and

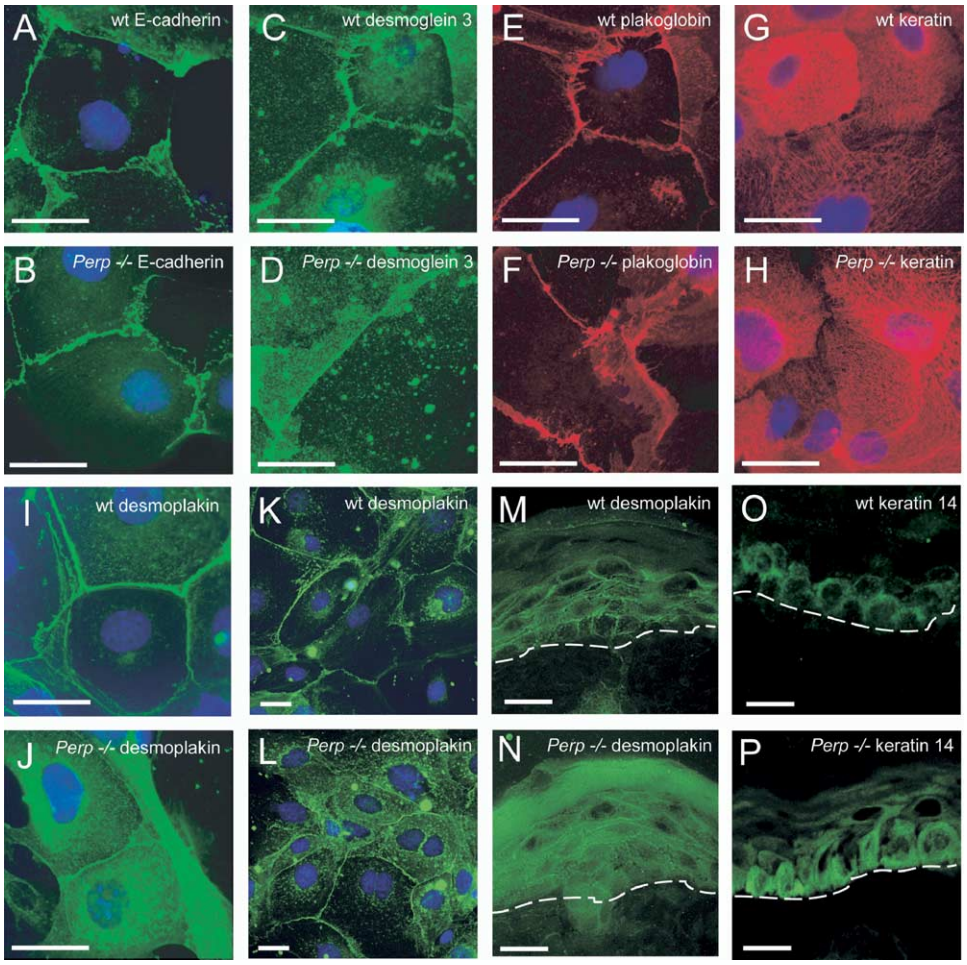

Figure 6. Desmoplakin Localization Is Abnormal in *Perp*$^{-/-}$ Keratinocytes

(A–L) Examination of desmosomal protein localization in keratinocytes derived from wild-type and *Perp*$^{-/-}$ mouse skin.

(A and B) Adherens junction formation (marked by E-cadherin localization) is unaltered in *Perp*$^{-/-}$ keratinocytes.

(C and D) Similarly, desmoglein 3 localizes normally in *Perp*$^{-/-}$ keratinocytes.

(E and F) Localization of plakoglobin appears normal in *Perp*$^{-/-}$ keratinocytes.

(G and H) Keratin intermediate filaments appear normal in *Perp*$^{-/-}$ keratinocytes when compared to wild-type cells.

(I and J) Localization of the desmosomal plaque protein desmoplakin (DP) is significantly altered in *Perp*$^{-/-}$ cells. Whereas DP typically localizes to the plasma membrane in wild-type keratinocytes (I), a significant fraction of DP in *Perp*$^{-/-}$ cells remains in the cytoplasm (J).

(K and L) This difference is evident widely in the population through a low-power view.

(M and N) This difference may also be detected in *Perp*$^{-/-}$ skin, where a greater fraction of DP is distributed within the cells (N) rather than localizing to the membrane as in wild-type skin (M).

(O and P) *Perp*$^{-/-}$ skin also exhibits abnormal keratin 14 aggregation (P) when compared to wild-type skin (O).

7B), the localization of most desmosomal proteins, including desmoglein 3 and plakoglobin, was largely unaltered in *Perp*$^{-/-}$ keratinocytes (Figures 6C–6F). In contrast, the staining pattern for desmoplakin appeared different from that seen in wild-type cells (Figures 6I–6L). Whereas most desmoplakin localized to the cell membrane in adherent wild-type keratinocytes, desmoplakin exhibited diffuse intracellular staining with minimal plasma membrane targeting in *Perp*$^{-/-}$ keratinocytes.

Although the increase in cytoplasmic desmoplakin could result from the higher protein levels present in *Perp*$^{-/-}$ cells, the fact that other overexpressed desmosomal components target appropriately to the plasma membrane supports the idea that there may be a specific defect in desmoplakin localization. Consistent with our results in this keratinocyte model, we found that in skin from wild-type and *Perp*$^{-/-}$ newborn mice, desmoglein 3 and plakoglobin localized primarily to the cell periphery while desmoplakin showed some cytoplasmic retention and keratin 14 aggregated abnormally within the cell (Figures S5C–S5F and Figures 6M–6P). In the skin, desmoplakin levels are not affected by *Perp* deficiency, further suggesting that this is not the only basis for the mislocalization observed in keratinocytes. Finally, examination of E-cadherin and actin staining revealed that formation of adherens junctions in *Perp*$^{-/-}$ keratinocytes and skin appears unaltered, underscoring the specific effect of Perp loss on desmosomes (Figures 6A, 6B, S5A, and S5B and data not shown).

We next determined the relative amounts and solubility profiles of desmosomal components in wild-type and *Perp*$^{-/-}$ skin. Examination of total desmosomal pro-

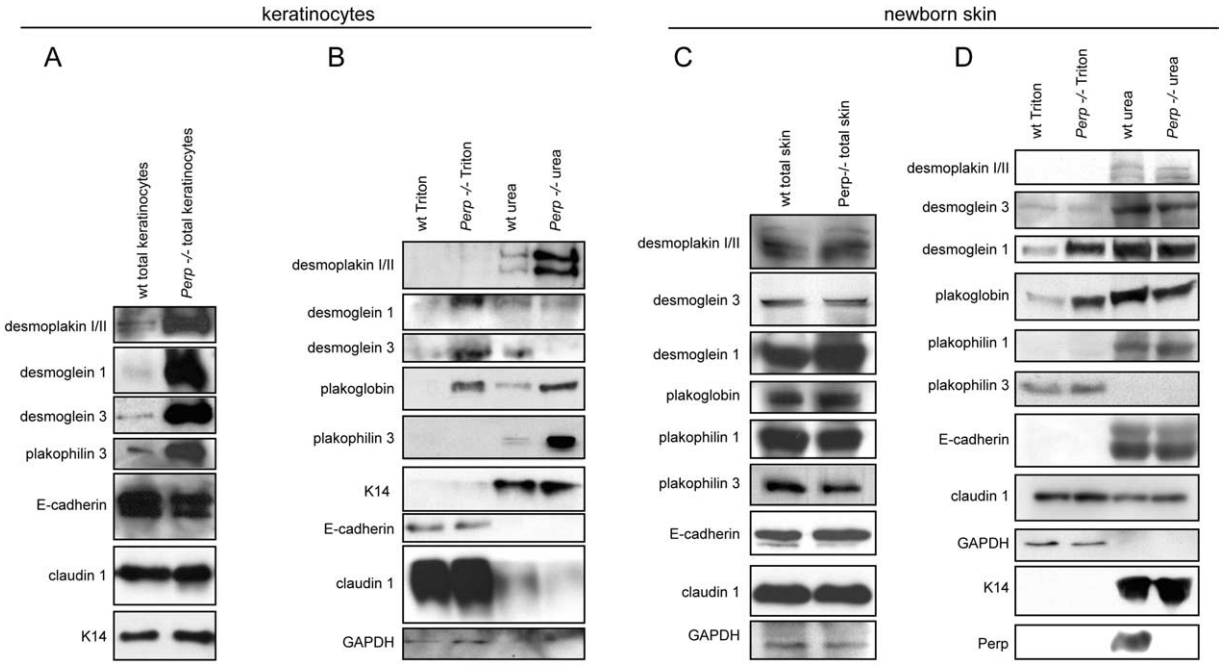

Figure 7. Desmosomal Protein Solubility Is Perturbed in *Perp*$^{-/-}$ Mouse Skin

(A) Western blot analysis demonstrates that desmosomal proteins are present at higher levels in total protein extracts from *Perp*$^{-/-}$ keratinocytes compared to wild-type keratinocytes, whereas nondesmosomal proteins are unaffected. K14 serves as a loading control.

(B) Enhanced Triton X-100 solubility is observed for the desmosomal proteins desmoglein 1, desmoglein 3, and plakoglobin in fractions derived from *Perp*$^{-/-}$ keratinocytes and analyzed by Western blot. E-cadherin and claudin 1 show similar solubility in wild-type and *Perp*$^{-/-}$ keratinocytes. GAPDH and K14 serve as loading controls for the Triton X-100-soluble and -insoluble fractions, respectively.

(C) Desmosomal proteins are present at approximately equal levels in wild-type and *Perp*$^{-/-}$ total mouse skin, as determined by Western blot analysis. The adherens junction protein E-cadherin and the tight junction protein claudin 1 are also unaffected.

(D) Triton X-100 solubility profiles of desmosomal proteins in wild-type and *Perp*$^{-/-}$ mouse skin. Desmogleins 1 and 3 and plakoglobin are enriched in the Triton X-100 soluble fraction from *Perp*$^{-/-}$ skin. This effect is specific to desmosomal constituents, as E-cadherin and claudin 1 are unaffected.

tein levels demonstrated that there is no significant alteration of protein levels in *Perp*$^{-/-}$ skin relative to wild-type skin (Figure 7C). We then determined which proteins could be extracted by Triton X-100 and which could be solubilized only by chaotropic agents, the classic behavior for assembled desmosomal proteins (Bornslaeger et al., 2001; Vasioukhin et al., 2001). Interestingly, we observed that Perp partitioned into the urea fraction, similar to other desmosome-associated proteins, supporting the idea that Perp is a desmosomal constituent (Figure 7D). Furthermore, we found that some desmosome proteins, specifically desmoglein 1 and plakoglobin, are greatly enriched and desmoglein 3 levels are slightly enhanced in the Triton X-100-soluble fraction from *Perp*$^{-/-}$ skin relative to wild-type skin (Figure 7D). Although total protein levels of desmosomal constituents were higher in cultured keratinocytes from *Perp*$^{-/-}$ mice than those from wild-type mice, suggesting adaptation to culture conditions in the absence of Perp, the pattern of altered solubility was similar to that seen in skin (Figures 7A and 7B). Together, these findings indicate that the fraction of proteins efficiently incorporated into the desmosome is diminished in *Perp*$^{-/-}$ epithelia, supporting a role for Perp in desmosome assembly or stability. Such a defect also explains the less electron-dense appearance and increased width of desmosomes detected in *Perp*$^{-/-}$ skin compared to wild-type skin by EM. These solubility effects appear to be specific to desmosomes, as the adherens junction and tight junction components E-cadherin and claudin 1 displayed unaltered properties in *Perp*$^{-/-}$ skin and keratinocytes (Figures 7A–7D).

These data collectively support a role for Perp in proper desmosome function. As desmoplakin is required to link the desmosomal plaque to the keratin intermediate filament cytoskeleton, any abnormal cytoplasmic accumulation in *Perp*$^{-/-}$ cells suggests a possible rationale for the lack of attachment of desmosomes to the cytoskeleton observed by EM. Additionally, although plakoglobin and the desmogleins apparently target to the plasma membrane, their increased solubility in *Perp*$^{-/-}$ cells and skin relative to wild-type controls suggests that despite proper localization, they may not be correctly incorporated into desmosomes. The decreased stability of desmosomal complexes provides a basis for the observed malfunction of desmosomes in *Perp*$^{-/-}$ epithelia and underscores the central role for Perp in desmosome function and epithelial integrity.

Discussion

Perp Is a p63-Regulated Gene

Here, through analysis of knockout mice lacking the p53 apoptosis-associated target gene *Perp*, we reveal a fundamental role for Perp in promoting cell-cell adhe-

sion and maintaining epithelial integrity. The phenotype of *Perp*$^{-/-}$ mice, which display severe blisters in tissues prone to stress as well as postnatal lethality, contrasts with the viability of *p53*$^{-/-}$ mice, indicating a p53-independent developmental function for Perp. This result, along with several other findings, implicates Perp instead in a pathway downstream of the p53-related protein p63 in the process of stratified epithelial development. First, the observation that *p63* and *Perp* have very similar expression profiles in E9.5–10.5 embryos and in a variety of stratified epithelia in older animals initially suggested that *Perp* may be directly regulated by p63. Second, like Perp, p63 plays a crucial part in the establishment of stratified epithelia, including the skin and oral mucosa, although the role of p63 is more global and the role for Perp more specialized. p63 is necessary for the genesis of stratified epithelia, as demonstrated by the absence of these structures in *p63*$^{-/-}$ mice (Mills et al., 1999; Yang et al., 1999). Moreover, expression of p63 is sufficient to induce simple epithelia to express markers of stratified epithelia, illustrating that p63 acts as a master switch directing the initiation of epithelial stratification (Koster et al., 2004). As part of this process, p63-mediated induction of a transcriptional program specifying stratified epithelial development likely includes activation of a set of genes involved in epithelial specialization, such as *Perp*.

Consistent with the notion of a p63-Perp pathway, we have demonstrated here that *Perp* expression in the developing embryo and in cultured keratinocytes depends on p63. That p63 directly induces *Perp* is demonstrated by reporter assays and chromatin immunoprecipitation experiments showing p63 binding to the *Perp* regulatory region in vivo. Furthermore, we show that all p63 isoforms examined, including both TA and ΔN isoforms, are competent to activate expression of the *Perp* luciferase reporter. Although the exact roles of the multiple p63 isoforms in vivo are incompletely understood, it is proposed that they have distinct roles during skin development, with TAp63 and ΔNp63 playing roles in commitment to stratification during embryogenesis and epidermal differentiation in mature skin, respectively (McKeon, 2004; Koster et al., 2004). Our data suggest that *Perp* is regulated by more than one p63 isoform in the skin, which may reflect a broad requirement for Perp at different times during stratified epithelial development as well as in all layers of the tissues specified by p63. The prevailing notion is that ΔNp63 isoforms act primarily to inhibit p53 or p63 target gene activation. Our results, along with other recent studies (Ellisen et al., 2002), indicate that the scenario is more complex than originally appreciated: ΔNp63 is not simply a negative regulator but retains activity to stimulate expression of certain genes. This suggests that there may be different classes of p63 target genes that respond differentially to the various isoforms of p63, as a reflection of their biological function. Perp is a target gene that can be activated by all isoforms of p63 and is induced at multiple stages of development, consistent with the requirement for proper adhesion throughout development. Thus, Perp is the first p63 target with a demonstrated functional role consistent with regulation by both sets of isoforms, including the ΔNp63 isoforms thought to predominate in the mature skin (McKeon, 2004).

These studies identify *Perp* induction as a critical subprogram in the specification of stratified epithelia by p63. The mode by which p63 specifies skin development is controversial, with roles either in stem cell maintenance or in commitment to stratification being proposed. Our findings support a model in which p63, during induction of a stratification program, transactivates a cohort of genes that endow a stratified epithelium with specific characteristics rather than simply maintaining the epidermal proliferative compartment.

Perp Plays a Central Role in Stratified Epithelial Integrity by Promoting Desmosome Assembly

Perp's specific role within the framework of the p63 developmental program for stratified epithelia is in establishing cell-cell adhesive contacts. In particular, Perp localizes to desmosomes and is required for proper desmosome formation in stratified epithelia, as demonstrated by the abnormal morphology of desmosomes and the altered properties of desmosomal components in *Perp*$^{-/-}$ skin. Given the association of compromised desmosome function with various human skin disorders (Green and Gaudry, 2000), these results suggest the tantalizing possibility that *Perp* mutations may be implicated in human blistering diseases of unknown etiology.

Two general models may explain how Perp might participate in desmosome assembly and function. Perp's contribution to desmosomal integrity could be as a core structural component or, alternately, as a chaperone that facilitates the transit of other critical desmosome components to the plasma membrane. Some desmosomal constituents, such as the transmembrane desmosomal cadherin molecules, which engage in heterotypic interactions between neighboring cells and nucleate the desmosomal plaque protein complex at the cytoplasmic face of the cell, are clearly involved in establishing the architecture of the desmosome (Garrod et al., 2002). Likewise, Perp could participate either in homotypic or heterotypic interactions at the plasma membrane to provide important adhesive contacts that constitute part of the desmosomal framework. Another potential structural role for Perp is as an anchoring point for connections to the intermediate filament cytoskeleton.

As a chaperone, Perp might assist in the trafficking or assembly of desmosomal subunits. In the case of adherens junction complexes, β-catenin acts as a molecular chauffeur for E-cadherin, facilitating its shuttling from the secretory pathway to the plasma membrane (Chen et al., 1999). Examination of the migration of desmosome components to the plasma membrane has suggested that the desmosomal cadherins and desmoplakin transit to the plasma membrane through two different compartments and assemble to form the desmosome after reaching the membrane (Getsios et al., 2004). In particular, desmoplakin has been described to localize to discrete packets in the cytosol and to travel to the cell surface via the intermediate filament network upon receiving the proper cue (Green and Gaudry, 2000). Plakophilin 1 participates in the recruitment of desmoplakin to the plasma membrane, as skin cells from patients with Plakophilin 1 mutations display cytoplasmic desmoplakin localization and defects in des-

mosomal plaque-intermediate filament connections (Bornslaeger et al., 2001; McMillan et al., 2003). However, other facets of this assembly and trafficking process are as yet uncharacterized, leaving open the possibility that Perp may participate in these events.

There is precedent for tetraspan proteins acting as molecular escorts or organizing factors for membrane proteins. For example, stargazin, a member of the claudin/PMP-22/EMP family, is implicated in the delivery of the AMPA receptor to the plasma membrane of cerebellar granular neurons, as well as in the clustering of these receptors at the synapse (Chen et al., 2000). This scenario is likely to be paradigmatic for tetraspan membrane proteins, in which they actively promote transiting, organization, or stabilization of plasma membrane proteins into complexes essential for effecting specific cellular processes. We envision that Perp likewise may play a role in the shuttling, assembly, or stabilization of desmosomal proteins.

Perp Is Important for Tissue Homeostasis Downstream of Both p63 and p53

Our findings invite speculation about the connection between Perp's roles in apoptosis and adhesion. While the mechanism by which Perp participates in p53-mediated apoptosis is not well understood, its activities in programmed cell death and adhesion may share common features. Perp activity in each of these processes may reflect a shared cell biological role that is relevant to both cellular responses or, alternatively, a signaling role that differs according to developmental context. A general function for Perp could relate to the shuttling or assembly of membrane proteins at the plasma membrane: death receptors in the case of apoptosis and adhesion components in the case of desmosomes. Alternatively, Perp may utilize distinct activities to enable the apoptotic and adhesion responses. In the future, identification of functional domains within Perp will help determine whether both activities are dependent on a common motif or different regions of this multifaceted protein.

In its roles downstream of both p53 and p63, Perp is implicated in signaling important for tissue integrity. The p53 tumor suppressor is known as a "guardian of the tissue," with an essential function in maintaining tissue homeostasis (Attardi and Jacks, 1999). In response to cellular stresses including DNA damage or hyperproliferative signals, p53 induces apoptosis, in part through Perp, as a measure to protect an organism against malignancy (Vousden and Lu, 2002). Similarly, the p63-Perp axis may be involved in the establishment or maintenance of tissue integrity, in this case by facilitating appropriate cell-cell contacts necessary for tissue function. The p53 and p63 pathways may intersect to integrate signals that control tissue homeostasis in different settings, in some cases through apoptosis, in some cases through adhesion. We propose the existence of signaling complexes that sense the local environment and thereby promote either apoptosis or adhesion, with Perp playing a key role in both processes.

Experimental Procedures

In Situ Hybridization

In situ hybridization with digoxigenin- or ^{35}S-radiolabeled probes was carried out as described, using a probe transcribed from a plasmid containing the full-length *Perp* cDNA (pT7T3Pac-mPerp) (Frantz et al., 1994; Yang et al., 1999). For section in situ hybridization, 6 μm frozen sections from E16.5 embryos were used.

Northern Blot Analysis

RNA samples were isolated from snap-frozen tissue or cultured cells using Trizol (Invitrogen). Northern blotting was performed according to standard methods.

Retroviral Infection of Primary Keratinocytes

Retroviruses were produced by transiently transfecting Phoenix-E cells (G. Nolan, Stanford University) with constructs expressing shRNA targeting exon 4 of *p63* (p63 hairpin 1, or D8, antisense target sequence: GACTGCTGGAAGGACACATCGAAGCTGTG; pMSCVpuro-ZZ-SHAG-LICaka4A), exon 6 of *p63* (p63 hairpin 2, or D9, antisense target sequence: GTGATAGGATCTTCTACATACTGGGCATG), or with a GFP-expressing control (pMSCV-puro-PIG; Hemann et al., 2003), as described. Infections were performed as described (Hemann et al., 2003), and keratinocytes were cultured for 72–96 hr prior to RNA and protein harvesting.

Reporter Assays

50,000 *p53*$^{-/-}$;*p63*$^{-/-}$ MEFs or primary human keratinocytes were plated in wells of a 24-well plate. The next day, cells were transiently transfected using Fugene 6 (Roche) with 250 ng of empty vector (pcDNA3.1), a p53 expression vector (pCMVp53WT; Reczek et al., 2003), or vectors encoding the indicated p63 isoforms (Yang et al., 1998) and 250 ng of either the pPerpLucPS reporter construct or pPerpLucPSmutD (Reczek et al., 2003) as well as 25 ng of pRLnull (Promega). After 24 hr, cells were harvested and luciferase activity was measured using the Dual-Luciferase Reporter Assay system (Promega). Firefly luciferase values were divided by Renilla luciferase values to control for transfection efficiency. Each experiment was performed at least three times, with duplicate samples in each experiment.

Chromatin Immunoprecipitation

Chromatin was prepared by isolating P1.5 skin and fixing immediately in formaldehyde for 10 min. A single-cell suspension was made from fixed skin, cells and nuclei were lysed, and chromatin was sonicated to an average length of 800 bp before incubation with the 4A4 anti-p63 antibody (Santa Cruz) or an isotype control nonspecific antibody. After immunoprecipitation with protein A/protein G beads (Pharmacia), crosslinks were reversed and isolated DNA was used for PCR with primers flanking the *Perp* p53/p63 consensus site D (Reczek et al., 2003) or primers for an irrelevant region of *Perp* not containing a consensus site.

Adenoviral Infection

p63$^{-/-}$ cultured E18.5 ectoderm cells were plated for 48 hr after isolation. Cells were infected with Ad-pShuttle-CMV-TAp63γ or Ad-pShuttle-CMV (Ellisen et al., 2002) for 2 hr. Cells were harvested for protein and RNA at 24 and 36 hr after infection, respectively.

Histology and Immunohistochemistry

Paraffin sections from newborn and P7.5 mice were prepared for immunohistochemical or hematoxylin/eosin staining by standard methods. Immunohistochemistry was performed according to standard methods, with permeabilization for antigen retrieval by microwaving in 0.01 M citrate buffer (pH 6.0) or 1M Tris (pH 9.5), 5% urea buffer.

EM and Image Analysis

For immunogold labeling, ventral skin sections were taken from P0.5 mice and embedded in Lowicryl K4M resin at –35°C, sectioned, and mounted on nickel grids before labeling with anti-Perp antibodies and colloidal gold-conjugated secondary antibodies. For transmission EM, pieces of tongue and ventral skin were taken from P0.5 newborn mice and prepared by standard methods. Sections were imaged on a JEOL TEM 1230 microscope with a Gatan 967 CCD camera (Stanford Electron Microscopy Core).

Desmosome properties in 50,000× magnification EM images were quantified as follows: total continuous membrane length and individual desmosome length along the plasma membrane were

measured and normalized against the scale bar within each image. Individual desmosomes were scored for electron density as light (plasma membrane visible) or dark (not possible to see membrane), attachment to intermediate filaments, and as normal or abnormal based on the above characteristics or detachment from apposed cells. Measurements were compiled for statistical analysis using GraphPad Prism.

Protein Preparation and Immunoblotting

For skin protein preparation, skin was snap-frozen and homogenized using a chilled mortar and pestle. For keratinocyte protein preparation, plated cells were washed with PBS and chilled buffer was added. For Triton-soluble protein fractions, cells or skin samples were resuspended in 1% Triton X-100 solubilization buffer (Vasioukhin et al., 2001), rocked for one hour at 4°C, and the supernatant was isolated by centrifugation. The urea-soluble protein fraction was obtained by resuspending the Triton-insoluble material from this preparation in the same buffer +9M urea. Total protein extracts were made by direct lysis in 9M urea buffer. Western blotting was performed according to standard methods, with 25–50 μg of protein in each lane.

Keratinocyte Culture and Adhesion Assays

E18.5 *p63*$^{-/-}$ ectoderm or skins from P0.5 mice were prepared as described (Koster et al., 2004), pooled by genotype, and plated in DMEM containing 1.2 mM calcium, fetal calf serum (FCS), and growth factor supplements. For calcium-dependent adhesion assays, cells were washed three times with Ca^{2+}-free PBS the next day and refed with EMEM containing 8% dialyzed FCS, antibiotics, and 0.05 mM Ca^{2+}. Cells were grown to ~80% confluency, washed with PBS, and incubated in the same media with 1.2 mM Ca^{2+} to induce epithelial sheet formation. After 48 hr, cells were harvested for protein extracts or immunofluorescence.

Immunofluorescence

Keratinocytes cultured on 35 mm plates with sterile glass coverslips were fixed in either cold 2% paraformaldehyde in PBS for 20 min or in chilled methanol for 5 min. Samples of skin from newborn mice were prepared by embedding the specimens in OCT. Five to seven micrometer frozen sections were fixed 5 min in 1:1 methanol:acetone and allowed to air dry. Immunofluorescence was done as described (Attardi et al., 2000).

Antibodies

For immunofluorescence and immunohistochemistry, we used antibodies against Ki67 (Pharmingen), desmoplakin I/II (RDI), desmoglein 1 (4B2, gift of K. Green, Northwestern), desmoglein 3 (gift of J. Stanley, University of Pennsylvania), E-cadherin (Zymed), plakoglobin (1407, gift of K. Green, Northwestern), ZO-1 (gift of W.J. Nelson, Stanford), plakophilin 1 (RDI), keratins 14, 1, and 6, and loricrin (Covance). For immunoblotting, we also used antibodies against p63 (4A4, Santa Cruz), desmoglein 3 (Santa Cruz), claudin 1 and plakophilin 3 (Zymed), and GAPDH (RDI). Polyclonal antibodies against Perp were generated by injection of a carboxy-terminal peptide fragment ((C)NYEDDLLGAAKPRYFY, Zymed), and affinity purified by coupling the peptide to Sulfolink resin (Pierce) following the manufacturer's directions.

Supplemental Data

Supplemental Data include five figures and Supplemental Experimental Procedures and can be found with this article online at http://www.cell.com/cgi/content/full/120/6/843/DC1/.

Acknowledgments

We would like to thank S. Artandi, J. Sage, J.M. Irish, W.J. Nelson, P. Jackson, A. Brunet, P. Khavari, and A. Oro for helpful discussions and critical reading of the manuscript. We are grateful to K. Green, J. Stanley, and W.J. Nelson for providing antibodies. We would also like to thank C. Thut, D. Zinyk, and C. Kaznowski for assistance with in situ hybridization, J. Perrino for EM staining, R. Vogelmann, K. Siemers, and T. Perez for advice and reagents for filter staining assays and microscopy, K. Bernot for instruction in keratinocyte culture, and L. Ellisen for the gift of p63 adenoviruses. This work was supported by the NCI (PHS Grant Number CA09302) to R.A.I. and by the NCI (CA93665-01) and Damon Runyon Cancer Research Foundation to L.D.A.

Received: July 29, 2004
Revised: November 2, 2004
Accepted: January 6, 2005
Published: March 24, 2005

References

Attardi, L.D., and Jacks, T. (1999). The role of p53 in tumour suppression: lessons from mouse models. Cell. Mol. Life Sci. *55*, 48–63.

Attardi, L.D., Reczek, E.E., Cosmas, C., Demicco, E.G., McCurrach, M.E., Lowe, S.W., and Jacks, T. (2000). PERP, an apoptosis-associated target of p53, is a novel member of the PMP-22/gas3 family. Genes Dev. *14*, 704–718.

Bornslaeger, E.A., Godsel, L.M., Corcoran, C.M., Park, J.K., Hatzfeld, M., Kowalczyk, A.P., and Green, K.J. (2001). Plakophilin 1 interferes with plakoglobin binding to desmoplakin, yet together with plakoglobin promotes clustering of desmosomal plaque complexes at cell-cell borders. J. Cell Sci. *114*, 727–738.

Chen, Y.T., Stewart, D.B., and Nelson, W.J. (1999). Coupling assembly of the E-cadherin/beta-catenin complex to efficient endoplasmic reticulum exit and basal-lateral membrane targeting of E-cadherin in polarized MDCK cells. J. Cell Biol. *144*, 687–699.

Chen, L., Chetkovich, D.M., Petralia, R.S., Sweeney, N.T., Kawasaki, Y., Wenthold, R.J., Bredt, D.S., and Nicoll, R.A. (2000). Stargazin regulates synaptic targeting of AMPA receptors by two distinct mechanisms. Nature *408*, 936–943.

Dohn, M., Zhang, S., and Chen, X. (2001). p63alpha and DeltaNp63alpha can induce cell cycle arrest and apoptosis and differentially regulate p53 target genes. Oncogene *20*, 3193–3205.

Ellisen, L.W., Ramsayer, K.D., Johannessen, C.M., Yang, A., Beppu, H., Minda, K., Oliner, J.D., McKeon, F., and Haber, D.A. (2002). REDD1, a developmentally regulated transcriptional target of p63 and p53, links p63 to regulation of reactive oxygen species. Mol. Cell *10*, 995–1005.

Flores, E.R., Tsai, K.Y., Crowley, D., Sengupta, S., Yang, A., McKeon, F., and Jacks, T. (2002). p63 and p73 are required for p53-dependent apoptosis in response to DNA damage. Nature *416*, 560–564.

Frantz, G.D., Weimann, J.M., Levin, M.E., and McConnell, S.K. (1994). Otx1 and Otx2 define layers and regions in developing cerebral cortex and cerebellum. J. Neurosci. *14*, 5725–5740.

Fuchs, E., and Raghavan, S. (2002). Getting under the skin of epidermal morphogenesis. Nat. Rev. Genet. *3*, 199–209.

Garrod, D.R., Merritt, A.J., and Nie, Z. (2002). Desmosomal cadherins. Curr. Opin. Cell Biol. *14*, 537–545.

Getsios, S., Huen, A.C., and Green, K.J. (2004). Working out the strength and flexibility of desmosomes. Nat. Rev. Mol. Cell Biol. *5*, 271–281.

Green, K.J., and Gaudry, C.A. (2000). Are desmosomes more than tethers for intermediate filaments? Nat. Rev. Mol. Cell Biol. *1*, 208–216.

Hemann, M.T., Fridman, J.S., Zilfou, J.T., Hernando, E., Paddison, P.J., Cordon-Cardo, C., Hannon, G.J., and Lowe, S.W. (2003). An epi-allelic series of p53 hypomorphs created by stable RNAi produces distinct tumor phenotypes in vivo. Nat. Genet. *33*, 396–400.

Ihrie, R.A., Reczek, E., Horner, J.S., Khachatrian, L., Sage, J., Jacks, T., and Attardi, L.D. (2003). Perp is a mediator of p53-dependent apoptosis in diverse cell types. Curr. Biol. *13*, 1985–1990.

Jetten, A.M., and Suter, U. (2000). The peripheral myelin protein 22 and epithelial membrane protein family. Prog. Nucleic Acid Res. Mol. Biol. *64*, 97–129.

Koch, P.J., Mahoney, M.G., Ishikawa, H., Pulkkinen, L., Uitto, J., Shultz, L., Murphy, G.F., Whitaker-Menezes, D., and Stanley, J.R. (1997). Targeted disruption of the pemphigus vulgaris antigen (des-

moglein 3) gene in mice causes loss of keratinocyte cell adhesion with a phenotype similar to pemphigus vulgaris. J. Cell Biol. *137*, 1091–1102.

Koster, M.I., Kim, S., Mills, A.A., DeMayo, F.J., and Roop, D.R. (2004). p63 is the molecular switch for initiation of an epithelial stratification program. Genes Dev. *18*, 126–131.

Kurata, S., Okuyama, T., Osada, M., Watanabe, T., Tomimori, Y., Sato, S., Iwai, A., Tsuji, T., Ikawa, Y., and Katoh, I. (2004). p51/p63 controls subunit alpha3 of the major epidermis integrin anchoring the stem cells to the niche. J. Biol. Chem. *279*, 50069–50077.

McKeon, F. (2004). p63 and the epithelial stem cell: more than status quo? Genes Dev. *18*, 465–469.

McMillan, J.R., Haftek, M., Akiyama, M., South, A.P., Perrot, H., McGrath, J.A., Eady, R.A., and Shimizu, H. (2003). Alterations in desmosome size and number coincide with the loss of keratinocyte cohesion in skin with homozygous and heterozygous defects in the desmosomal protein plakophilin 1. J. Invest. Dermatol. *121*, 96–103.

Mills, A.A., Zheng, B., Wang, X.J., Vogel, H., Roop, D.R., and Bradley, A. (1999). p63 is a p53 homologue required for limb and epidermal morphogenesis. Nature *398*, 708–713.

Reczek, E.E., Flores, E.R., Tsay, A.S., Attardi, L.D., and Jacks, T. (2003). Multiple response elements and differential p53 binding control Perp expression during apoptosis. Mol. Cancer Res. *1*, 1048–1057.

South, A.P., Wan, H., Stone, M.G., Dopping-Hepenstal, P.J., Purkis, P.E., Marshall, J.F., Leigh, I.M., Eady, R.A., Hart, I.R., and McGrath, J.A. (2003). Lack of plakophilin 1 increases keratinocyte migration and reduces desmosome stability. J. Cell Sci. *116*, 3303–3314.

Tsukita, S., and Furuse, M. (2002). Claudin-based barrier in simple and stratified cellular sheets. Curr. Opin. Cell Biol. *14*, 531–536.

Vasioukhin, V., Bowers, E., Bauer, C., Degenstein, L., and Fuchs, E. (2001). Desmoplakin is essential in epidermal sheet formation. Nat. Cell Biol. *3*, 1076–1085.

Vousden, K.H., and Lu, X. (2002). Live or let die: the cell's response to p53. Nat. Rev. Cancer *2*, 594–604.

Wong, P., Colucci-Guyon, E., Takahashi, K., Gu, C., Babinet, C., and Coulombe, P.A. (2000). Introducing a null mutation in the mouse K6alpha and K6beta genes reveals their essential structural role in the oral mucosa. J. Cell Biol. *150*, 921–928.

Yang, A., Kaghad, M., Wang, Y., Gillett, E., Fleming, M.D., Dotsch, V., Andrews, N.C., Caput, D., and McKeon, F. (1998). p63, a p53 homolog at 3q27–29, encodes multiple products with transactivating, death-inducing, and dominant-negative activities. Mol. Cell *2*, 305–316.

Yang, A., Schweitzer, R., Sun, D., Kaghad, M., Walker, N., Bronson, R.T., Tabin, C., Sharpe, A., Caput, D., Crum, C., and McKeon, F. (1999). p63 is essential for regenerative proliferation in limb, craniofacial and epithelial development. Nature *398*, 714–718.

Yeaman, C., Grindstaff, K.K., and Nelson, W.J. (2004). Mechanism of recruiting Sec6/8 (exocyst) complex to the apical junctional complex during polarization of epithelial cells. J. Cell Sci. *117*, 559–570.